Available online at www.sciencedirect.com
ScienceDirect
Physics Procedia 78 (2015) 328 – 336
Physics Procedia

15th Nordic Laser Materials Processing Conference, Nolamp 15, 25-27 August 2015, Lappeenranta, Finland

Selective Laser Melting of Polymer Powder – Part mechanics as function of exposure speed

Maximilian Drexler[a,b]*, Matthias Lexow[b] , Dietmar Drummer[a,b]

[a]*Collaborative Research Center 814 – Additive Manufacturing (CRC 814), Am Weichselgarten 9, 91058 Erlangen, Germany*
[b]*Friedrich-Alexander-University Erlangen-Nürnberg (FAU), Institute of Polymer Technology, Am Weichselgarten 9, 91058 Erlangen, Germany*

Abstract

The selective laser melting of polymer powders is a well-established technology for additive manufacturing applications, although there is still a deficit in basic process knowledge. Considering the demands of series production, the technique of selective laser melting of polymers is faced with various challenges concerning suitable material systems, process strategies and part properties. Consequently, basic research is necessary to understand and optimize processes in order to enable a shift from prototyping applications to serial production of small-lot sized series. A better understanding of the interaction between the sub-processes of selective laser melting and the resulting part properties is necessary for the derivation of new process strategies for increased part quality. Selective laser melting of polymers is mainly divided in the three phases of powder feeding, tempering and geometry exposure. By the interaction of these sub-processes, the resulting temperature fields determine the part properties through microstructural changes in the pore number and distribution. In addition to absolute temperature values, the time dependency of the thermal fields has an influence on the porosity of the molten parts. Current process strategies aim for a decrease in building time by increasing scan speed and laser power, although the absolute energy input into the material does not change when scan speed and laser power are increased at a constant ratio. In prior investigations, the authors showed a correlation between the heating rate and the shape of the resulting melt pool. Based on this correlation, the interaction between heating rates (on a fixed level of exposure energy) and mechanical part properties (tensile test) is analyzed within the paper. The study also implies additional results for other levels of energy input during geometry exposure, which allow for a cross-check of the results. Furthermore, part positioning in the build chamber as well as part density are taken into account. Based on these basic investigations, new process strategies considering the time dependent material behavior can be derived.

Peer-review under responsibility of the Lappeenranta University of Technology (LUT)

Keywords: Selective laser melting; heating rate; part density; tensile properties

* Maximilian Drexler. Tel.: +49-9131-8529717 ; fax: +49-9131-8529709 .
E-mail address: drexler@lkt.uni-erlangen.de

Peer-review under responsibility of the Lappeenranta University of Technology (LUT)
doi:10.1016/j.phpro.2015.11.047

1. Motivation and state of the art

Techniques of additive manufacturing are established for prototyping applications, due to their unlimited freedom of design. Part production directly out of a digital part model without any additional molds offers a straight way from part construction to part production. Consequently, additive manufacturing processes are currently used for a vast number of new application fields, especially in branches requiring short development times or high part complexity (Kruth et al., 2005 and Caulfield et al., 2007 and Wohlers, 2011).

Besides design applications, especially for technical parts, products made by additive manufacturing processes have increased in importance, now being more than mere demonstration objects (Rietzel, 2008). Despite the huge variety of additive manufacturing processes only a few of them have the potential to meet the requirements of industrial manufacturing processes for small-lot sized series. Considering industrial requirements (e.g. mechanical strength of parts, reproducibility of part properties), one of the most promising additive processes is the selective laser melting (SLM) of mostly semi-crystalline thermoplastic powders (Wendel et al., 2008). The different sub-processes of SLM are shown in Fig. 1.

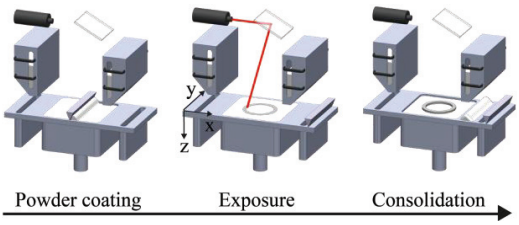

Fig. 1. Selective laser melting process (SLM) of thermoplastic polymer powder.

To meet the requirements of an industrial production, the sub-processes (powder coating, exposure, material consolidation) of the selective laser melting process and their mutual interactions (e.g. melt-pool-dimensions and energy input) are investigated experimentally and transferred into models. Based on this basic research and based on process modeling of newly adapted process strategies for improved part as well as process quality can be developed. Due to this fact, the potential of selective laser melting can be opened up also for serial manufacturing of highly individualized products (Kühnlein et al., 2011 and Rietzel et al., 2011).

Currently available processing strategies aim to perform the part building process by using higher scan speeds and laser powers while keeping the volume energy input into a layer at a constant value. This practice is based on the estimation that equal energy input (experimentally derived for each material) into the powder bed results in equal melt pool dimensions and part properties. Hereby, the speed of energy input into the powder bed is commonly neglected, although time dependent behavior of semi-crystalline polymers is well known from other polymer processing technologies. In the following, the authors will investigate time-dependent effects on part mechanics. Therefore, within different energy levels varying exposure speeds are investigated with respect to their effect on the mechanical part properties. Consequently, effects related to the time dependency of energy input can be faced. Based on these investigations the time-dependent behavior can be exploited for new exposure strategies within the selective laser melting process.

Nomenclature

c_p	specific heat capacity
d_f	spot size of the laser beam
d_L	thickness of the powder layer
δ_{opt}	optical penetration depth of the laser beam
E_D	energy density
ε_{break}	elongation at break

H	heating rate
h_s	hatch distance during exposure
l_t	distance for surface roughness measurement
m	mass
n	number of samples
P_L	power of the laser beam
R_Z	average maximum height of profile (surface roughness)
ρ_{part}	density of the part
σ_{max}	tensile strength
T	temperature
T_B	temperature of the build chamber
t	time
v_s	scan speed of the laser beam
v_t	speed of the roller during the coating phase

2. Experimental setup

2.1. Laser Melting System (LMS)

To guarantee constant experimental boundary conditions between different experiments, it is necessary to use a special temperature stabilized and homogenized laser melting system (LMS). Due to a multiple heating zone system within the used LMS, the whole building chamber is nearly equally tempered (approximately ± 5 K over the building area of 300 x 300 mm^2). This means, disturbing effects caused by temperature variation (e.g. local variations in part density) within the building chamber can be minimized. Moreover, a laser system with constant spot size d_f of the laser beam over the whole building chamber is used (F-Theta lens). The scanning system is cutting edge and guarantees short acceleration times as well as high precision in beam guiding. The focus diameter d_f is set to 400 μm. Due to the very short exposure times (0.12 - 0.51 ms) within the design of experiments the heating of the optical gating system is avoided. This means that the Gaussian beam profile is very stable for different exposure parameters.

2.2. Specimens

The specimens are type A tensile bars according to EN ISO 3167 scaled with a ratio of 1:2 in size (Fig. 2a) and built with various combinations of scan speed v_s and laser power P_L. Between the different experiments, the ratio between P_L and v_s is kept constant. According to Drexler et al. (2014) the energy density E_D, which is input into a single layer, can be approximated with Eq. 1. Within this equation the thickness of the exposed layer d_L (≈100 μm) as well as the hatching distance h_s (≈250 μm) can be assumed to be constant. (Nöken, 1997 and Keller, 1998)

$$E_D = \frac{P_L}{d_L \cdot h_s \cdot v_s} \tag{1}$$

In Eq. 1 it is obvious that for a constant ratio P_L/v_s also the energy density E_D remains unchanged. Nevertheless, the speed of the energy input changes. This can be expressed by the so-called heating rate, which can be approximated by Eq. 2, according to Drexler et al. (2014). The heating rate is a well-known parameter in polymer science and allows for a direct comparison between the laser melting process and standard laboratory analysis, e.g. differential scanning calorimetry (DSC).

$$H = \frac{P_L}{m \cdot c_p} = \frac{dT}{dt} \tag{2}$$

For the determination of the mechanical properties, i.e. tensile strength and elongation at break, the built tensile bars are characterized by tensile tests. According to DIN EN ISO 527-1, -2 the testing speed is set to 2.5 mm/min. The tensile bars are in dry condition.

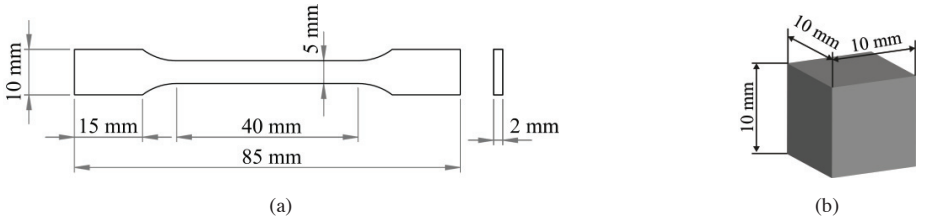

Fig. 2. (a) Scaled tensile bar and (b) cubic specimen.

Aside from tensile bars, cubes (Fig. 2b) are manufactured with the same processing parameters as the tensile bars. Due to their simple shape the cubes are used for analyzing the part density as function of part positioning and processing parameters. The density of the cube samples is determined with the immersion method according to DIN EN ISO 1183 in ethanol. The generally expected problem of a possible alteration of the buoyancy by air bubbles at the rough surface (Kühnlein, 2013) was found to be negligible within the investigations as was already noted in prior investigations by Drexler et al. (2014). In order to detect variations in part density in relation to the positioning, the cubes are distributed over the whole building area. Fig. 3b schematically shows the positioning of the cubes. All building processes are done at a constant temperature of the building chamber $T_B = 173$ °C and a hatch distance of $h_s = 250$ μm. The powder is coated by a roller system with constant coating parameters (coating speed $v_t = 250$ mm/s and amount of coated material), to minimize disturbing effects caused by the coating system (Kühnlein et al., 2012 and Drexler et al., 2014). In order to achieve nearly constant material properties for the whole experiment, standard laser melting powder, PA12 (type: PA2200, EOS GmbH, Krailling, Germany), is used. A technical mixture of material is processed: refreshed powder consisting of 50 % virgin PA12 and 50 % recycled powder (as typically used in the industry).

2.3. Microscopy

In addition to tensile tests also microscopic analysis of the fracture surface is performed with a scanning electron microscope (SEM) Zeiss Ultra Plus with a field emission source and an acceleration of 10 kV. For the topographic measurement secondary electrons are detected. The samples' surfaces are sputtered-coated with platinum/gold prior to the investigation. From the appearance of the fracture surfaces the fracture behavior can be derived by identifying brittle and ductile areas as well as defects (e.g. vacuoles) in layer connection.

2.4. Surface Roughness

The surface roughness of the tensile specimens is determined with a contact profilometer. The tip diameter of the diamond stylus is 5 μm. The results are given according to ISO 4287 as the average maximum height of profile represented by the R_z value. The distance for each measurement is $l_t = 4$ mm and located at the middle of the test bars.

2.5. Design of experiments (DoE)

Table 1 shows the design of experiments. The values for laser power P_L and scan speed v_s are chosen based on industrially used parameters while maintaining two levels of constant energy input during exposure.

Table 1. Design of Experiments (DoE).

	Process parameters		
	Laser power P_L	***Energy density E_D***	***Scan speed v_s***
	[W]	***[J/mm³]***	***[mm/s]***
1	6.00	0.3	800
2	13.50		1,800
3	21.00		2,800
4	24.75		3,300
5	8.00	0.4	800
6	18.00		1,800
7	28.00		2,800
8	33.00		3,300

3. Results and discussion

3.1. Part density

The density of beam molten parts is assumed to be influenced by local inhomogeneities of the thermal fields within the beam melting process. In turn, the density influences the mechanical behavior of a laser molten part. Due to these facts it was necessary to isolate variations in part density caused by different positioning in the building chamber. Fig. 3 shows the density distribution of cubic specimens as function of local positioning in the build area.

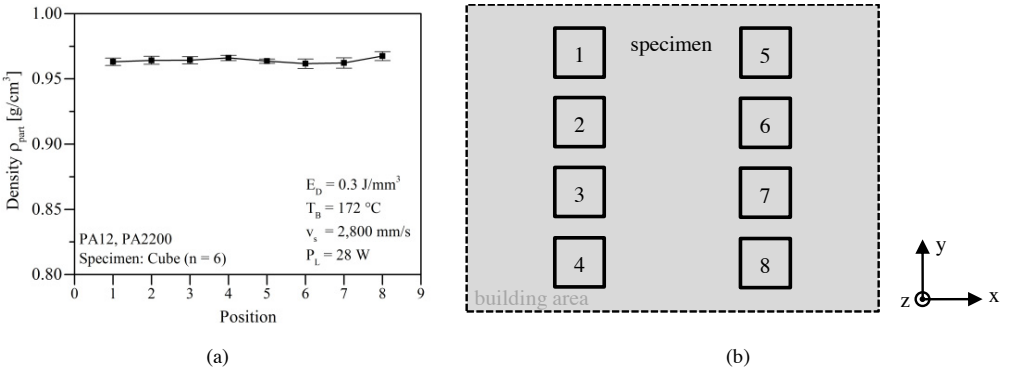

Fig. 3. (a) Density distribution over the building chamber; (b) positioning of cubic specimens in the building area.

Fig. 3 defines the boundary conditions for the presented experimental results. It shows, that within the experiments the density was nearly independent from the position in the building area, especially when the standard deviation is taken into account. By this reason, the variations in density shown below are the result of changes in the processing parameters, in particular changes in exposure speed. Furthermore, the stability of density over the building area is an indication for a homogenious temperature field of the LMS as well as an indication for a homogenious powder coating process. Consequently, within the applied LMS, experimental boundary conditions seem to be constant for analyzing time dependent effects on part level. Fig. 4 shows the part density as function of heating speed for a lower energy density $E_D = 0.3$ J/mm³.

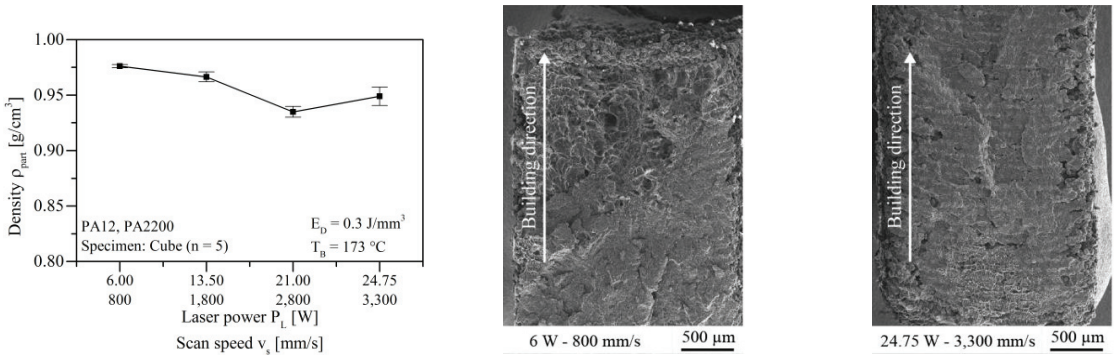

(a) (b) (c)

Fig. 4. (a) Part density as function of exposure speed; (b) fracture surface for low and (c) for high exposure speed at E_D = 0.3 J/mm³.

According to Fig. 4a, for higher P_L and v_s (i.e. higher exposure speed at constant E_D) the density of the molten parts declined for the investigated energy level E_D = 0.3 J/mm³. A reason for the decline might be the relatively low level of energy input E_D = 0.3 J/mm³ in relation to the high speed of energy input. As known from prior investigations the depth of the melt pool declines for higher exposure speeds (Drexler et al., 2014). Furthermore, for a low level of energy input E_D the size of the melt pool is reduced. The combination of these two circumstances results in a reduced density for increased exposure speeds. The decrease in density is visible in the microscopic images of the fracture surfaces of the tested tensile bars. Fig. 4b shows no borderlines between coated layers in building direction, which is an indication for a dense connection between the layers and thus a homogenious melt pool after the exposure. Contrarily, for an increased exposure speed (on constant level of E_D = 0.3 J/mm³) borderlines between single layers are clearly visible (Fig. 4c). The reason for this behavior might be the reduced melting depth for increased exposure speed. Due to minimized impact times nearly no heat conduction into the surrounding powder is possible. Consequently, absorbed laser energy is distributed only over exposed particles within the optical penetration depth δ_{opt} where most of the laser's intensity is extenuated. This means, particles within the penetrated zone are molten predominantly. Furthermore, the limited time for a thermal conduction into z-direction during exposure (especially for short impact times) results in a heat accumulation at the exposed surface, as described by Drexler et al. (2014 and 2015). Additionally, the high temperatures reached during exposure promote decomposition effects within the polymeric material. Furthermore, if the heat accumulates next to the surface more energy is released through radiation from the exposed area into the ambient, i.e. the building chamber. These mechanisms result in a decrease of effectively absorbed laser power and thus a reduced melt depth for the higher exposure speeds. In combination with a low absolute energy input E_D the acquired melt depth is not deep enough for a dense part and a strong connection between the layers, especially for a high scan speed.

For an increased level of absolute energy input E_D = 0.4 J/mm³ a constant density for the parts is obtained (Fig. 5a). In addition to the measured part densities, the SEM images of the fracture surfaces (Figs. 5b and 5c) indicate a fairly similar fracture behavior. In both cases no borderlines distinguishing single layers are observed, which indicates a sufficient melting depth even at a high laser scan speed.

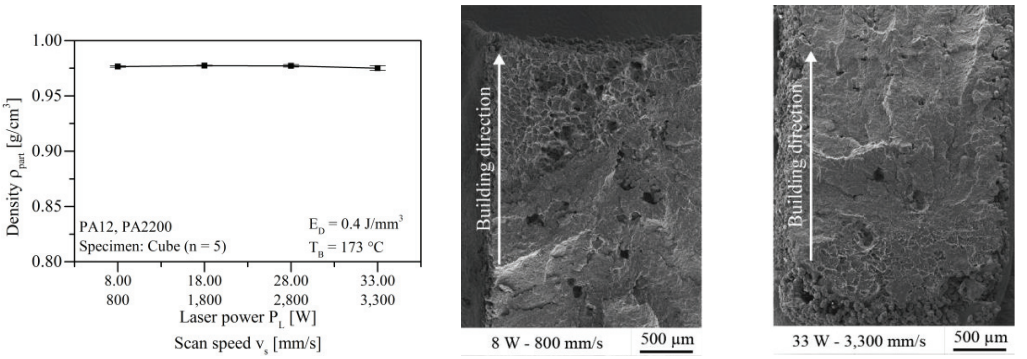

(a) (b) (c)

Fig. 5. (a) Part density as function of exposure speed; (b) fracture surface for low and (c) for high exposure speed at E_D = 0.4 J/mm³.

The reason for this behavior of the parts produced with a higher energy density is that the size of the melt pool for an increased level of energy input is generally larger, as described by Drexler et al. (2014).

3.2. Part Mechanics

The mechanical properties of laser molten parts are the result of the superposition of different factors based on material, process and part construction. Although the isolation of all superpositions is difficult, by investigation of different levels of absolute energy input E_D in addition to the variation of the speed of exposure the isolation of single effects is targeted. Also by this approach, time dependent effects can be seperated from energy dependent effects. Especially this consideration distinguishes this study from other, partly cited scientific work.

Fig. 6a shows the tensile properties of the bars manufactured with E_D = 0.3 J/mm³ as a function of exposure speed. With increasing exposure speed elongation at break ε_{break} as well as tensile strength σ_{max} decrease. This could be the result of an interaction between the part density behavior and resulting mechanical properties explained above. A weak strength of the connection between layers for a high exposure speed (Figs. 4b and 4c) also results in decreasing tensile strength and elongation at break.

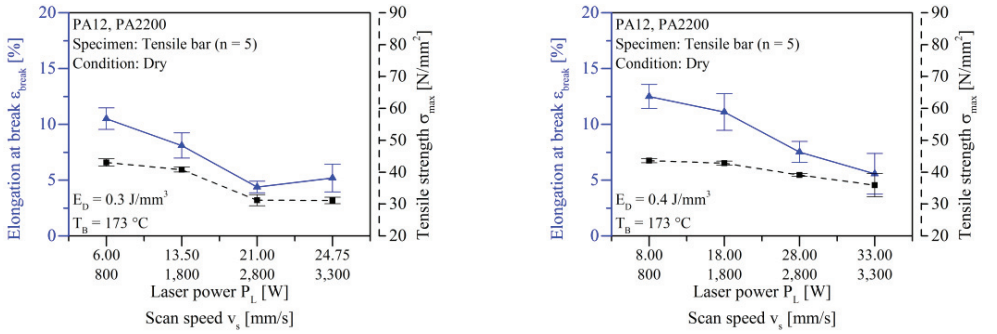

(a) (b)

Fig. 6. Tensile properties as function of exposure speed for an energy level of (a) E_D = 0.3 J/mm³ and (b) E_D = 0.4 J/mm³.

Fig. 6a shows the tensile properties for different exposure speeds for an increased level of energy input E_D = 0.4 J/mm³. The obtained values for elongation at break and tensile strength are only a little higher for this level of energy input than for E_D = 0.3 J/mm³, although usually the elongation at break is more sensitive, especially

concerning changes in material structure (Wudy et al., 2014). An increase in exposure speed leads to higher surface temperatures during exposure due to a heat accumulation based on the limited amount of time for heat conduction into the powder bed. Depending on the heating rate, the surface temperature can rise to values well above 420 °C for short periods of time (Drexler et al., 2014). The high intermediate temperatures are likely to induce thermal degradation which could be an explanation for the decline in elongation at break towards a higher scan speed. Another theory, introduced by Zarringhalam et al. (2008 and 2009), is based on the incomplete melting of the polymer particles, determined by the degree of particle melt (DPM). This leads to the initiation of cracks at the unmolten particles and thusly contributes to the explanation of the inferior mechanical properties of the sintered parts. An effect relating to the induction of post condensation as reported by Wudy et al. (2014) at the high intermediate temperatures is possible but probably minor at the relatively short time scale (Drexler et al., 2015). Alternative reasons for a decline in elongations, e.g. variation in density of specimens or poor layer connection, can be excluded with respect to Figs. 3 and 5. Crack initiation caused by surface roughness was considered not to be the crucial factor, as the different tensile specimens appear to have similar surface roughness conditions, see Fig. 7.

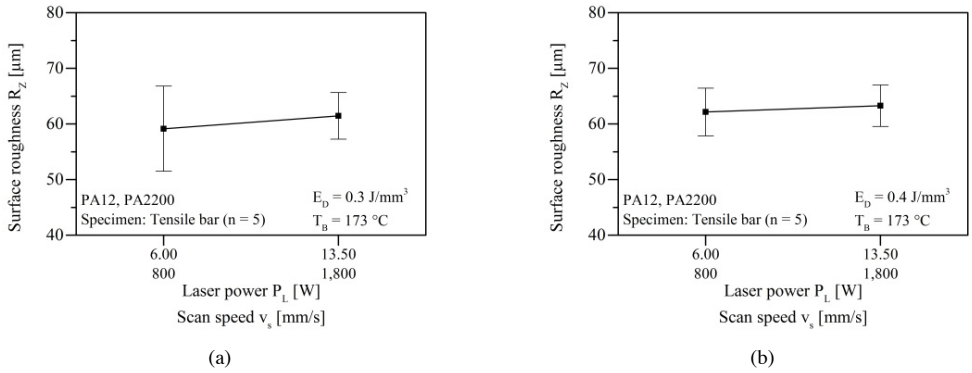

Fig. 7. Surface roughness of specimens manufactured with (a) 0.3 J/mm³ and (b) 0.4 J/mm³.

The results in Fig. 7 show that for an increasing heating speed as well as an increasing level of energy density no clear change in surface roughness appears. Consequently, crack initiation effects caused by surface roughness can be neglected within this study. Also, an adverse variance within the density measurement related to the surface roughness can be disregarded.

4. Summary and Conclusion

By a variation of the absolute energy input E_D during exposure, within values typically used in industrial applications, the authors could show, that the scan speed v_s can have an unfavorable influence on the part's mechanical properties, whereas the part density did not appear as the deciding factor. The boundary conditions for the experiments were defined through the density distribution in Fig. 3, determining the validity of the observations. Comparing the densities of specimens built with different levels of energy inputs E_D of 0.3 J/mm³ in Fig. 4 and 0.4 J/mm³ in Fig. 5, respectively, different dependencies on the scan speed were found. While at 0.3 J/mm³ the part density decreased with increasing scan speed, it remained constant for 0.4 J/mm³. An explanation was given with the SEM images of the respective fracture surfaces, revealing an insufficient melting depth for a high scan speed in the case of the lower value for E_D. However, indepently from the part density, the parts' mechanical properties, as shown in Fig. 6, decreased nonetheless in both cases with an increasing speed of energy input. The reason for this could be a change of the interaction between laser beam and polymer powder, resulting in a heat accumulation in the surface of the powder bed for very short impact times of the laser. Consequently, degradation processes could be induced which could in turn cause the decrease in the mechanical properties. A second explanation refers to the theory by Zarringhalam et al. (2009) based on the assumption that incomplete melting of the powder particles leads to centers of crack initiation.

The correlation of the results presented here with measurements of the DPM will be the subject of future work as it could allow for a distinct interpretation of the scan speed dependent material behavior. Concerning the process reliability and reproducibility of part properties, the shown scan speed dependent effects have to be recognized. An acceleration of the manufacturing speed through a decrease of the exposure time can lead to inferior part properties, even if the energy input E_D is kept constant.

Acknowledgements

The authors want to thank the German Research Foundation (DFG) for funding the Collaborative Research Centre 814 (CRC 814), sub-project B03.

References

Caulfield, B., McHugh, P.E., Lohfeld, S., 2007. Dependence of mechanical properties of polyamide components on build parameters in the SLS process. Journal of Materials Processing Technology, 182, 477-488.

Drexler, M., Wudy, K., Drummer, D., 2014. Derivation od Heating Rate Dependent Exposure Strategies for the Selective Laser Melting of Thermoplastic Polymers. Proceedings of the Polymer Processing Society 30th Annual Meeting, Cleveland, Ohio, USA.

Drexler, M., Wudy, K., Drummer, D., 2014. Resulting melt-pool-shape during selective beam melting of thermoplastics as function of energy input parameters. DDMC, Fraunhofer, Berlin.

Drexler, M., Wudy, K., Drummer, D., 2014. Density of laser molten parts as function of powder coating process during additive manufacturing. 7th World Congress on Particle Technology (WCPT7), Beijing.

Drexler, M., Wudy, K., Drummer, D., 2014. Derivation of heating rate dependent exposure strategies for the selective laser melting of thermoplastic polymers. 30th International Conference of the Polymer Processing Society, Cleveland, 2014.

Drexler, M., Wudy, K., Drummer, D., 2014. Impact of heating rate during exposure of laser molten parts on the processing window of PA12 powder. In: M. Schmidt, F. Vollertsen, M. Geiger (Eds.), Laser Assisted Net Shape Engineering 8 (LANE), Physics Procedia Elsevier B.V. Amsterdam, Fuerth.

Drexler, M., Wudy, K., Drummer, D., 2015. Interaction between Time Dependent Exposure Strategies and Part Positioning within Selective Laser Melting Process of Plastics. International Journal of Recent Contributions from Engineering, Science & IT (iJES), 3.

Keller, B., 1998. Grundlagen zum selektiven Lasersintern von Polymerpulver. Universität Stuttgart, Dissertation.

Kruth, J.P., Vandenbroucke, B., van Vaerenbergh, J., Mercelis, P., 2005. Benchmarking of different SLS/SLM processes as rapid manufacturing techniques. Int. Conf. Polymers & Moulds Innovations (PMI), Gent, Belgium, 2005.

Kühnlein, F., Drexler, M., Drummer, D., 2012. Effects on the density distribution of SLS-parts. Physics Procedia, 39, 500-508.

Kühnlein, F., 2013. Verarbeitung teilkristalliner Thermoplaste mittels selektivem Maskensintern. Friedrich-Alexander-Universität Erlangen-Nürnberg, Lehrstuhl für Kunststofftechnik, Dissertation.

Nöken, S., 1997. Technologie des Selektiven Lasersinterns von Thermoplasten. Rheinisch-Westfälische Technische Hochschule Aachen, Fakultät für Maschinenwesen, Dissertation.

Rietzel, D., Kühnlein, F., Feulner, R., Hülder, G., von Wilmowsky, C., Fruth, C., Nkenke, E., Schmachtenberg, E., 2008. Breaking Material Limitations in Selective Laser Sintering - An Opportunity for Medical Additive Processing. In: S.E.C.o.M. Polymers (Ed.), SPE European Conference on Medical Polymers, Belfast, UK, 61-65.

Rietzel, D., Drexler, M., Kühnlein, F., Drummer, D., 2011. Influence of temperature fields on the processing of polymer powders by means of laser and mask sintering technology. 22nd Annual International Solid Freeform Fabrication Symposium - An Additive Manufacturing Conference, SFF 2011, 252-262.

Rietzel, D., Drexler, M., Drummer, D., 2011. Grundlegende Betrachtungen zur Modellierung transienter thermischer Vorgänge beim selektiven Lasersintern von Thermoplasten. RTeJournal - Forum für Rapid Technologie, Erlangen.

Wendel, B., Rietzel, D., Kühnlein, F., Feulner, R., Hülder, G., Schmachtenberg, E., 2008. Additive Processing of Polymers. Macromolecular Materials and Engineering, 293.

Wohlers, T., 2011. Wohlers Report 2011 – State of the industry.

Wudy, K., Drexler, M., Drummer, D., 2014. Modelling of the Aging Behavior of Polyamide 12 powder during Laser Melting Process. International Conference of the Polymer Processing Society Cleveland, Ohio.

Zarringhalam, H., Majewski, N., Hopkinson, N., 2008. Effect of the degree of particle melt on mechanical properties in selective laser-sintered Nylon-12 parts. Proc. I. Mech. E., Part B: J. Engineering Manufacture, 222, 1055-1064.

Zarringhalam, H., Majewski, N., Hopkinson, N., 2009. Degree of particle melt in Nylon-12 selective laser-sintered parts. Rapid Prototyping Journal 15, 126-132.